Comparison between Measured Slab Profiles of Curled Pavements and Profiles Generated Using the Finite Element Method

Dr. Julie M. Vandenbossche[1], Member ISCP and Dr. Mark B. Snyder[2], Member ISCP

Abstract

The advancement in the processing speed of personal computers, as well as the more user-friendly graphical interfaces starting to be employed in pavement finite element analysis programs, has resulted in a more frequent use of the finite element method (FEM) for pavements analysis. This increase in reliance on the FEM has amplified the need to ensure these finite element models accurately predict the response of the slab to applied and environmental loads. This paper will focus on the ability of currently available finite element programs to accurately predict the response of rigid pavements to temperature gradients. The study entailed collecting surface profile measurements for a range of pavement designs under different temperature conditions. Each pavement design was then modeled using finite element analysis. Temperature gradients representing the conditions under which the slab profiles were measured were applied to the finite element models. Comparisons were then made between the measured and calculated slab shape. A comparison of the length of the unsupported portion of the slab determined using surface profile measurements and the FEM was performed. The FEM under-estimated the portion of the slab fully-supported only 12 percent of the time. The ability of the FEM to accurately estimate curvature appears to be a function of the pavement design and the magnitude of the gradient. Curvature was accurately determined using the FEM only 14 percent of the time with curvature being under-estimated 70 percent of the time. The FEM could not accurately estimate the larger curvatures. The curvatures calculated using slab profiles generated using the FEM tend to overestimate the curvatures calculated using measured profiles more frequently for thinner slabs and granular bases. The FEM predicted higher curvatures than were measured more frequently for unrestrained slabs than restrained.

Introduction

The advancement in the processing speed of personal computers, as well as the more user-friendly graphical interfaces starting to be employed in pavement finite element analysis programs, has resulted in a more frequent use of the finite element method (FEM) for pavements analysis. A new rigid pavement design procedure has recently been developed under the National Cooperative Research Program

[1] Julie M. Vandenbossche, Assistant Professor, Department of Civil and Environmental Engingeering, University of Pittsburgh, 3700 Ohara St., 934 Benedum Hall, Pittsburgh, PA, 15261, jmv@engr.pitt.edu
[2] Mark B. Snyder, Consultant, 6305 Oyster Bay Ct., Bridgeville, PA, 15017, markbsnyder@verizon.net

(NCHRP), 1-37A project. The FEM was also used, along with neural network concepts, to produce stress prediction equations for which transfer functions were developed for this new design procedure. This increase in reliance on the finite element method has amplified the need to ensure these finite element models accurately predict the response of the slab to applied and environmental loads. This paper will focus on the ability of currently available finite element programs to accurately predict the response of rigid pavements to temperature gradients.

The study entailed collecting surface profile measurements for a range of pavement designs under different temperature conditions. Each pavement design was then modeled using finite element analysis. Temperature gradients representing the conditions under which the slab profiles were measured were applied to the finite element models. Comparisons were then made between the measured and calculated slab shape.

Mn/ROAD Research Facility

Profile data collected at Mn/ROAD was used to evaluate the ability of the FEM to predict pavement response. Mn/ROAD is a densely-instrumented pavement test facility constructed adjacent to I-94 approximately 65 km (40 miles) northwest of Minneapolis, Minnesota. The mainline test road (MLR) is a 5.6-km (3.5-mile) segment of interstate that carries an average of 25,000 vehicles per day with approximately 12 percent truck traffic. The low volume test road (LVR) is a 4.0-km (2.5-mile) closed loop with a controlled weight and traffic volume that simulates conditions on rural roads.

This study includes data collected from the nine test cells that constitute the 5-year mainline and 10-year mainline concrete test sections, representing different combinations of slab thicknesses, joint spacings, restraint conditions, and subbase types. A detailed description of each test cell is provided in table 1. The measured material properties of the concrete used to construct each cell are summarized in table 2 and gradations of each base material is provided in table 3. Only jointed plain concrete pavements have been included in this study and all of the pavement designs contained asphalt shoulders. Pavement temperature and moisture, dipstick profile and falling weight deflectometer (FWD) deflection data were collected at the Mn/ROAD research facility.

The Mn/ROAD test cells provided data for model validation and calibration over the following variable ranges:

Summary of Design Variables

Pavement thickness	190 to 240 mm (7.5 to 9.5 in)
Transverse Joint Spacing	4.6 to 6.1 m (15 to 24 ft)
Panel widths	3.7 to 4.3 m (12 to 14 ft)
Foundation stiffness	49 to 77 kPa/mm (180 to 285 psi/in)
Drainage	Drained and undrained
Slab restraint	Doweled/tie bars and undoweled/no tie bars

Table 1. Summary of concrete test cell design features at Mn/ROAD.

Test Section	Cell	Slab Thickness mm (in)	Joint Spacing m (ft)	Lane Widths, Inside/Outside m (ft)	Dowel Diameter mm (in)	Base Type[1], Thickness, mm (in)	Edge Drains	Comments
5-Year	5	190 (7.5)	6.1 (20)	4.0/4.3 (13/14)	25 (1)	cl4sp, 75 (3) over cl3sp (68)	No	Dense graded base
5-Year	6	190 (7.5)	4.6 (15)	4.0/4.3 (13/14)	25 (1)	cl4sp, 125 (5)	No	Dense graded base
5-Year	7	190 (7.5)	6.1 (20)	4.0/4.3 (13/14)	25 (1)	PASB[2] 100 (4) over cl4sp, 75 (3)	Yes	
5-Year	8	190 (7.5)	4.6 (15)	4.0/4.0/4.3 (13/13/14)	25 (1)	PASB[2] 100 (4) over cl4sp, 75	Yes	3 lanes, transverse steel
5-Year	9	190 (7.5)	4.6 (15)	4.0/4.0/4.3 (13/13/14)	25 (1)	PASB,[2] 100 (4) over cl4sp, 75 (3)	Yes	3 lanes, no transverse steel
10-Year	10	240 (9.5)	6.1 (20)	3.7/3.7 (12/12)	32 (1.25)	PASB[2], 100 (4) over cl4sp, (75)	Yes	
10-Year	11	240 (9.5)	7.3 (24)	3.7/3.7 (12/12)	32 (1.25)	cl5sp, 125 (5)	No	Dense graded base
10-Year	12	240 (9.5)	4.6 (15)	3.7/3.7 (12/12)	32 (1.25)	cl5sp, 125 (5)	Yes	Dense graded base
10-Year	13	240 (9.5)	6.1 (20)	3.7/3.7 (12/12)	32 (1.25)	cl5sp, 125 (5)	No	Dense graded base

[1]See table 3.1.3 for the gradations of these materials or Mn/DOT 1995 Specifications.
[2] Permeable asphalt stabilized base (PASB)

Table 2. Summary of concrete mixture properties for test cells at Mn/ROAD.

Test Section	Cell	Unit Weight kg/m^3 (psi/ft^3)	Compressive Strengths (28-day) MPa (psi)	Modulus of Elasticity (28-day) MPa (psi)	Poisson's Ratio	Thermal Coefficient με/ °C (με/ °F)
5-Year	5	2390 (149)	36 (5215)	32,900 (4,800,000)	0.19	8.1 (4.5)
5-Year	6	2390 (149)	37 (5405)	33,900 (4,900,000)	0.19	8.1 (4.5)
5-Year	7	2395 (150)	36 (5205)	30,000 (4,400,000)	0.19	8.1 (4.5)
5-Year	8	2400 (150)	33 (4790)	31,800 (4,600,000)	0.19	8.4 (4.7)
5-Year	9	2385 (149)	37 (5430)	31,900 (4,600,000)	0.19	9.8 (5.4)
10-Year	10	2370 (148)	35 (5110)	28,800 (4,200,000)	0.19	8.1 (4.5)
10-Year	11	2405 (150)	39 (5590)	30,100 (4,400,000)	0.19	6.7 (3.7)
10-Year	12	2380 (149)	36 (5270)	30,100 (4,400,000)	0.21	8.8 (4.9)
10-Year	13	2370 (148)	34 (4885)	34,400 (5,000,000)	0.22	8.8 (4.9)

Table 3. Aggregate gradations (percent passing) for Mn/ROAD base materials.

	Base Material			
Sieve Size	cl3sp	Cl4sp	cl5sp	PASB
37.5-mm-(1-1/2-in)	--	100	--	--
31.5-mm (1-1/4-in)	--	--	--	100
25-mm (1-in)	--	95-100	100	95-100
19-mm (¾-in)	--	90-100	90-100	85-98
12.5-mm (½-in)	100	--	--	--
9.5-mm (3/8-in)	95-100	80-95	70-85	50-80
4.75-mm (No. 4)	85-100	70-85	55-70	20-50
2-mm (No. 10)	65-90	55-70	35-55	0-20
850-μm (No. 20)	--	--	--	0-8
425-μm (No. 40)	30-50	15-30	15-30	0-5
75-μm (No. 200)	8-15	5-10	3-8	0-3

1 in = 25.4 mm

Special crushing requirements (sp):

cl3sp and cl4sp: crushed/fractured particles are not allowed

cl5sp: 10-15 percent crushed/fractured particles are required.

Permeable asphalt stabilized base (PASB)

Initially, all test cells were constructed with dowels and tie bars; therefore, slab curling and warping could only be quantified under restrained slab conditions. While there are many concrete pavements built with load transfer devices, there are still pavements constructed which do not include them. The objective of this project involves quantifying the amount of curling and warping displayed by all concrete pavement slabs. Therefore, it was desirable to measure curling and warping deflections for slabs restrained by load transfer devices, as well as those not restrained. The dowel and tie bars were cored at the joint from one slab representing each pavement design in September 1995. The released slabs allow comparisons of curling/warping characteristics between restrained and unrestrained slabs under otherwise identical conditions.

The field data included in the study were collected during September 1995, April 1996 and October 1996. Data were collected at the Mn/ROAD research facility on three different occasions in an attempt to quantify seasonal effects. Each test period required 24-hour data collection to capture diurnal effects by collecting data for each test cell under zero, negative and positive gradient conditions.

Data Collection

Thermocouples were used to measure the temperature profile throughout the depth of the pavement structure. An automated system is established to collect temperature data every fifteen minutes. Surface profile measurements were made using a FACE dipstick (2). Dipstick measurements pertinent to this study were recorded along the diagonal of the slab. Each Dipstick run began and ended 10 cm (4 in) away from the approach transverse joint and 10 cm (4 in) away from the lane/shoulder longitudinal joint, as depicted in figure 1.

FWD testing was performed simultaneously with the dipstick measurements. FWD data was collected in the wheelpath and adjacent to the transverse joints to determine the deflection load transfer efficiency. The measured deflection load transfer efficiency was used to determine the stiffness of the joint in the finite element models. FWD testing was also performed in the corner of the slab where the dipstick runs initiated and at the geometric center of the slab. The modulus of subgrade reaction was backcalculated for each test cell using FWD deflection measurements made at mid-slab when the zero deformation gradient, or a gradient close to the zero deformation gradient, was present. Construction-related drying shrinkage and the slab setting when a temperature gradient is present produce a permanent deformation in the slab such that the slab will exhibit some deformation even when no temperature gradient exists. The zero-deformation gradient is the gradient condition that produces a flat slab profile. The backcalculated k-values were then used to quantify the support beneath the slab in the finite element models. Additional information on the collection and processing techniques used for the field data can be found in reference 4.

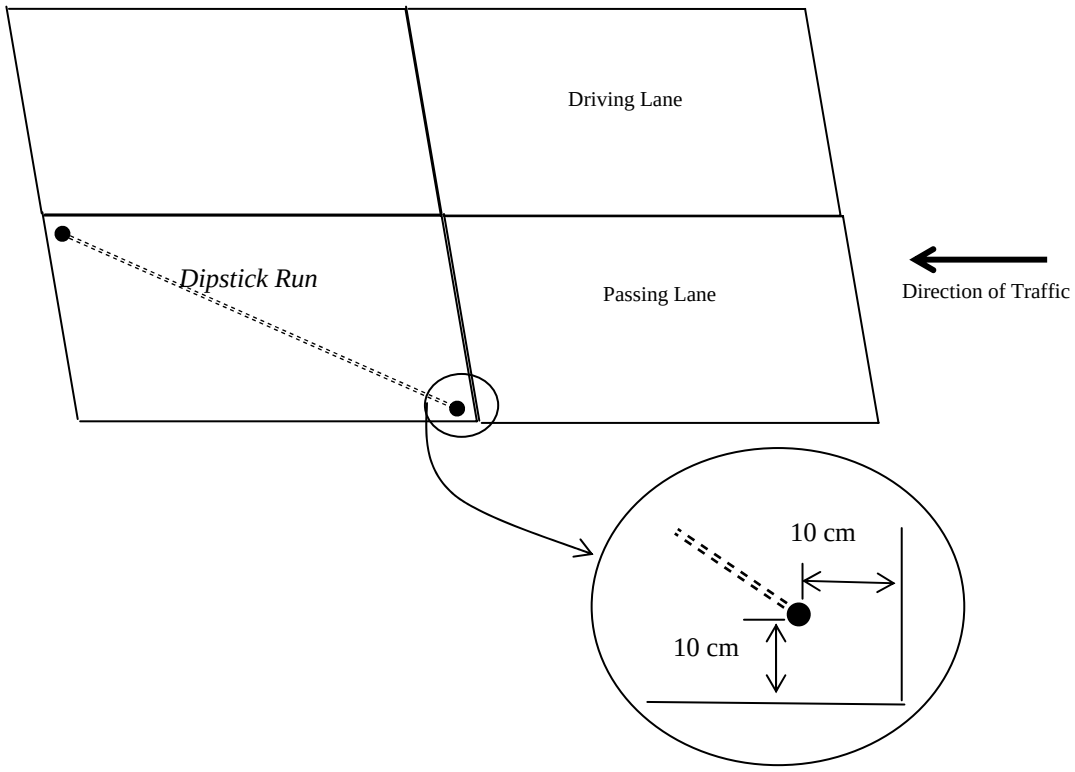

Figure 1. Location of dipstick run made during each data collection period.

Finite Element Modeling

A finite element model was constructed for each slab included in the study. The material properties and slab dimensions provided in tables 1 and 2 were used to develop the finite element models for each cell. Several modeling assumptions were made. It was assumed that medium-thick plate theory was applicable and that each pavement could be modeled as an equivalent two-layer system. The slab was constructed of one layer of elements with a mesh fineness of 15 cm x 15 cm (6 in x 6 in). The base layer in all test sections was modeled as an unbonded dense liquid foundation. The slab temperature profiles in the field were modeled in ISLAB200 using nonlinear temperature gradients with the temperature being defined at the top, middle and bottom of the slab. ISLAB2000 was the finite element pavement analysis program chosen for this study. This program was chosen because it is frequently used in the pavement community, it was used in the development of the 2002 Design Guide, it is user-friendly and the modeling assumptions inherent to this program are representative of those used in the majority of other finite element pavement analysis programs frequently used.

Finite element analyses were performed on the restrained and unrestrained slabs from which profile data were collected. Models representing the temperature profile conditions under which profile data was collected were developed for both positive and negative temperature gradients for each data collection period.

Analysis of Results

Due to the difficulty in using one variable to accurately define a non-linear gradient when graphing the response of the slab against the temperature profile throughout the depth of the slab, an equivalent linear gradient was calculated for each temperature profile. The equivalent linear gradient was only used for graphing purposes. As previously mentioned, the actual measured temperature profiles were used to model the nonlinear gradient in the finite element models and not the equivalent linear gradient. See work conducted by Janssen and Snyder for the calculation used in determining the equivalent linear temperature gradient (3). A direct comparison between the linear gradients and equivalent linear gradients estimated using this method along with the actual measured temperature profiles are provided in reference 4.

Comparisons were made between measured and predicted diagonal profiles for both restrained and unrestrained (when available) slabs in each test section. Eighty-one profiles were measured and compared to profiles generated using the FEM. Examples of graphs depicting these profiles are provided for an unrestrained and a restrained slab in Cell 7 in figures 2 and 3. The gradients provided in the legends of figures 2 and 3 represent the equivalent linear gradient. The measured profiles represent the difference between the shape of the slab at the time the profile was measured and the slab profile measured when no gradient was present. This provides a method for subtracting out the construction curling and warping and direct comparisons can then be made between the measured profiles and FEM. A complete set of all 81 profile measurements and the corresponding calculated profiles can be found in reference 4. The comparisons made between the FEM and measured slab profiles consisted of two components: 1) the length of the unsupported portion of the slab profile, and 2) the shape of the slab profile (see figure 4).

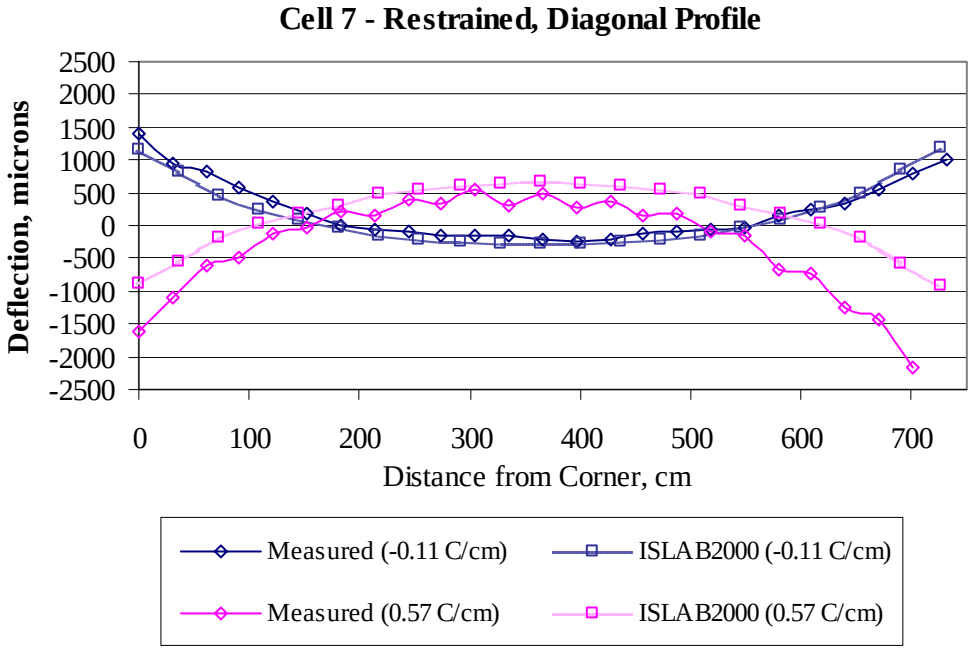

Figure 2. Comparison between measured and calculated surface profiles for a restrained slab in Cell 7.

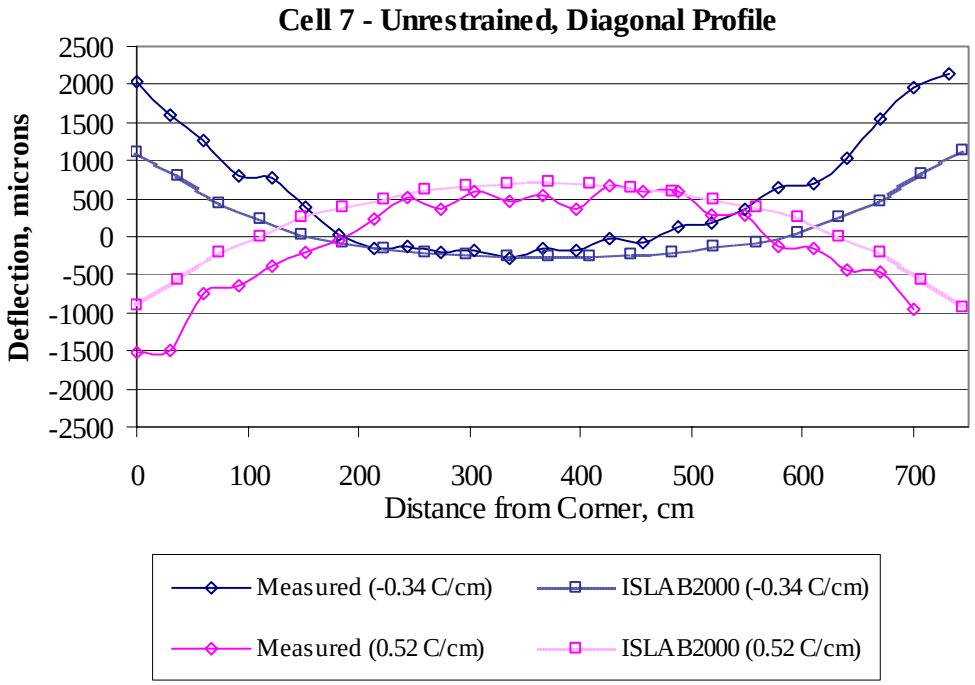

Figure 3. Comparison between measured and calculated surface profiles for the unrestrained slab in Cell 7.

A comparison of the length of the unsupported portion of the slab determined using surface profile measurements (labeled L_{MEAS} in figure 4.a.) and the FEM (labeled L_{FEM} in figure 4.a.) will be performed first. Typically L_{MEAS} and L_{FEM} were found to be approximately the same. Exceptions to this did occur for slabs in every test cell except Cells 5, 9, 10 and 11. For all of the other test cells, and both the restrained and unrestrained slabs in these test cells, the length of the supported portion of the slab (along the diagonal profile) was longer when estimated using the FEM than when profile measurements were made using the dipstick. This shift in the FEM profile from the measured profile only occurred when a large positive temperature gradient was present and was always upward, resulting in a larger portion of the FEM-modeled slab being unsupported when compared to the support conditions of the measured slab shape. In each case, the whole FEM profile was shifted upward away from the measured profile, which would indicate that the stiffness of the base (estimated as the backcalculated k-value) used in the FEM model was overestimated. Although, the FEM models using the same base stiffness for the same slab and data collection period but for a different gradient produce FEM profiles that accurately represent the measured profiles, indicating, that the assumed base stiffness is correct. An example of this is provided in figure 5. Figure 5 shows the profile measurements for two different temperature gradients (one positive and one negative) made in April 1996 for a slab in Cell 13, along with the profiles generated using the FEM. The same slab support conditions were assumed for both gradients. This indicates that current finite element programs might be over-

estimating how much of the slab is fully supported from some pavement designs when large positive gradients are present.

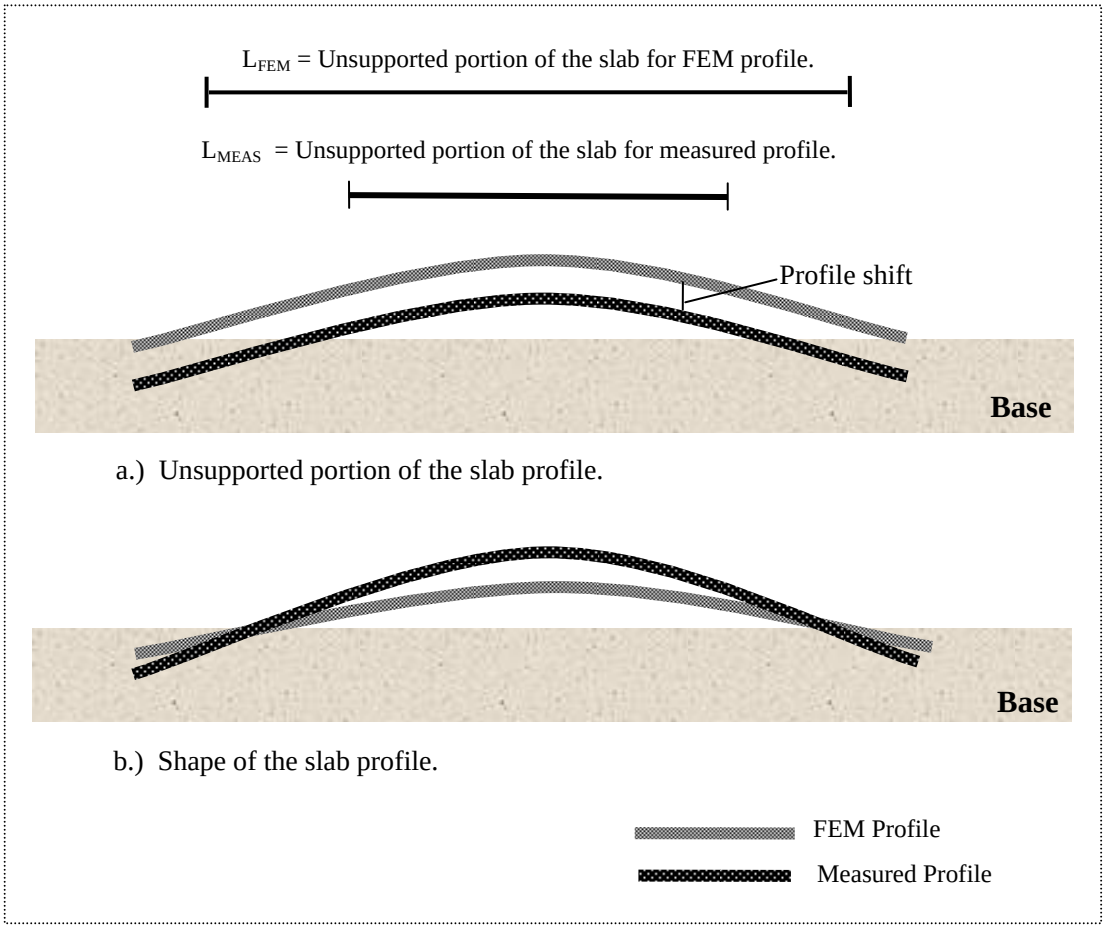

Figure 4. Comparisons between FEM and measured profiles; a) Unsupported portion of the slab profile. b.) Shape of the slab profile.

Only 12 percent of the FEM profiles were shifted upward from the measured slab profile. The shift in the profile was always less than 500 microns (20 mils). All equivalent linear temperature gradients were greater than +0.28 °C/cm (+1.28 °F/in) for slabs approximately 190 mm (7.5 in) thick and greater than +0.52 °C/cm (+2.31 °F/in) for slabs approximately 240 mm (9.5 in) thick when this phenomena was exhibited. An equivalent linear gradient greater than +0.28 °C/cm (+1.28 °F/in) is typically present more than 20 to 30 percent of the time based on 5-year temperature data for the slabs 190 mm (7.5 in) thick. A equivalent linear gradient greater than +0.52 °C/cm (+1.28 °F/in) is typically present more than 15 to 20 percent of the time based on 5-year temperature data for the slabs 240 mm (9.5 in) thick.

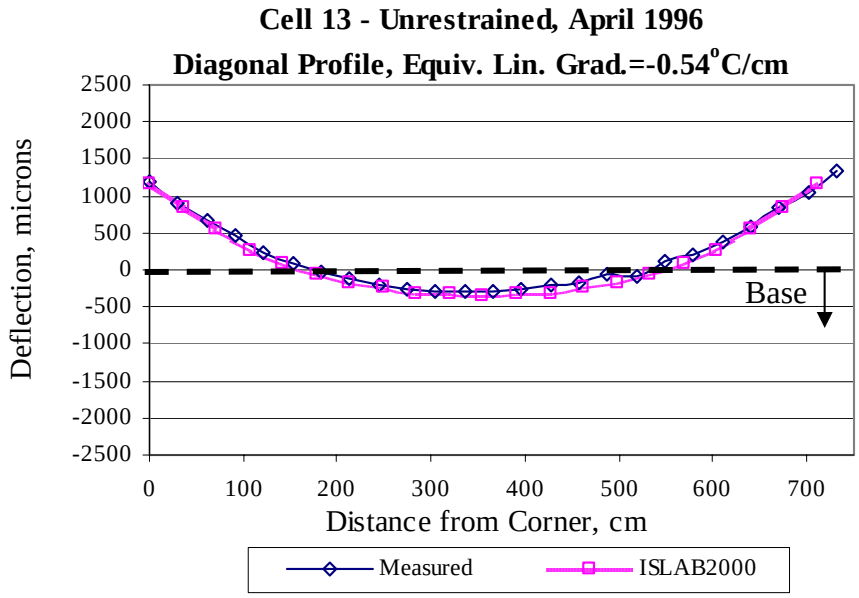

a.) Length of slab profile that is fully supported is the same for both measured and FEM profile.

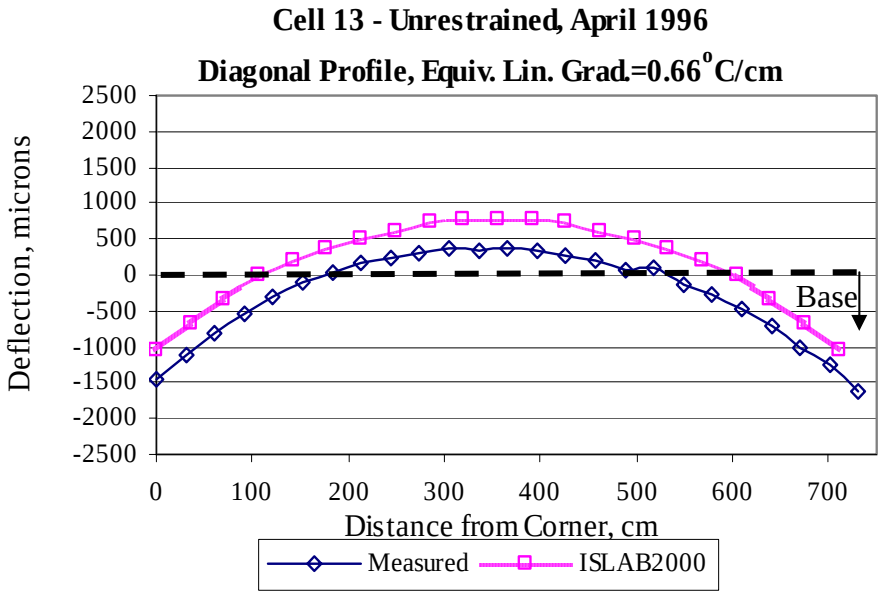

a.) Length of slab profile that is fully supported is not the same for both measured and FEM profile.

Figure 5. Length of slab profile that is fully supported is a) the same for both measured and FEM profile b) not the same for both measured and FEM profile.

This upward shift only occurred in a very small number of comparisons made between the measured profiles and the slab profiles estimated using the FEM. Unfortunately, it occurs when large positive gradients are present. This is the critical condition for the occurrence of bottom-up cracking. Further investigation should be made in determining how critical this inaccuracy is when estimating pavement life using the FEM.

The next step was to compare the shape of the slab profiles measured with those generated using the FEM. Identifying a single parameter that can characterize the measured profile, or slab shape, was required for making the comparisons. The parameter chosen to characterize the shape of the slab was curvature. To calculate curvature, the deflection equation for each surface profile must first be developed. An extremely good approximation of the surface profile was obtained using a second-order polynomial. Equations 1 and 2 were used for calculating the curvature of each measured profile and each profile generated using the FEM. After the second-order polynomial was fit to the diagonal profile, the curvature was calculated for each of the measured and FEM profiles.

$$\kappa = \frac{\frac{d^2 y}{d x^2}}{\left[1+\left(\frac{dy}{dx}\right)^2\right]^{\frac{3}{2}}} \qquad \text{Equation 1}$$

where:

$$y = A x^2 + Bx + C \qquad \text{Equation 2}$$

K = Curvature
y = Measured displacement
x = location along the profile traverse
A, B, and C = Coefficients

A quantitative comparison was made between the shape of the FEM and measured diagonal profiles by calculating the curvature for each profile. A graph of the curvatures calculated for the measured slab surface profiles and the profiles generated using the FEM is provided in figure 6. The graph shows the FEM does a better job predicting slab curvature when the curvature is small but is less accurate for larger curvatures. This trend is true regardless of weather the curvature is upward (positive) or downward (negative). The scatter of the data increases with increases in the magnitude of the curvature. Figure 7 shows the curvature plotted against its corresponding equivalent linear temperature gradient for both the measured profiles and the profiles generated using the FEM. It is shown that there is more scatter in the field measurements than the curvatures calculated using the FEM, as would be expected. This increase in scatter is also reflected in figure 6. Again, the scatter increases with increases in the magnitude of the curvature. The curvatures calculated for the field measurements match the curvatures calculated using the FEM generated surface profiles more closely when

small gradients are present but tend to increase at a faster rate with increasing gradients in both the positive and negative direction. The data indicates the FEM method more accurately predicts pavement curvatures when small gradients are present and tends to under-predict curvature when large positive or negative gradients are present. Neglecting construction curling/warping, creep and/or shrinkage in the finite element model would result in an under-prediction of positive curvature and an over prediction of negative curvature. The fact that the FEM is under-predicting both positive and negative curvature is an indication that subtracting the slab profile at a zero gradient condition from each measured profile was successful in negating the effects of curling/warping, creep and/or shrinkage.

A summary of the results of the comparison of the curvatures is provided in table 4. Curvatures were assumed to be approximately equal when the curvatures calculated using data from the FEM were accurate to +/-20 percent of the curvatures calculated using the measured surface profile data. Curvature was under-estimated by the FEM in 70 percent of the cases, with only a few instances where the FEM overestimated the measured curvature (16 percent). The FEM predicted higher curvatures than were measured more frequently for the restrained slabs than the unrestrained slab. Seventy-one percent of the curvatures overestimated by the FEM were negative. This indicates that the FEM is more likely to overestimate the curvature produce by a positive gradient than the curvature produced by a negative gradient. Based on the results of this study, the FEM is also more likely to estimate higher curvatures than the measured curvature when the curvature is small.

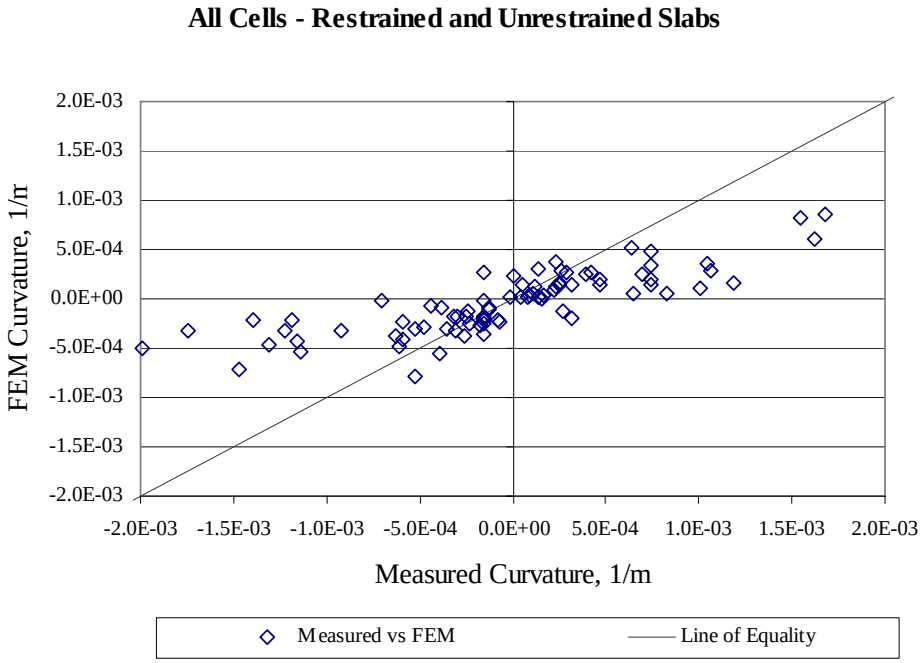

Figure 6. Curvatures of measured and finite element slab surface profiles the restrained and unrestrained slabs in each test cell.

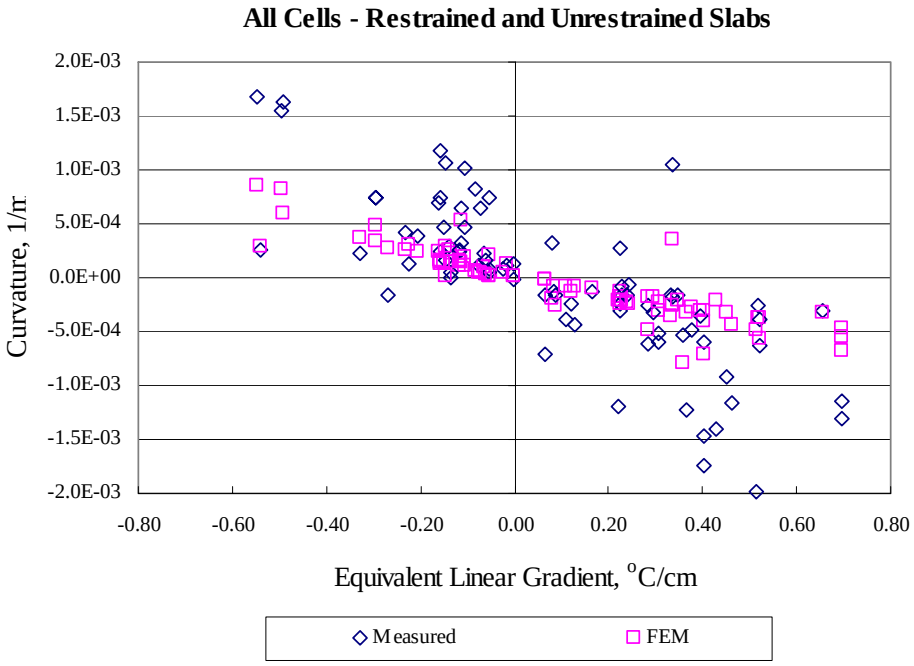

Figure 7. Curvatures of measured and finite element slab surface profiles plotted against the equivalent linear gradient under which it was measured.

Table 4. Summary of FEM and measured profile curvatures.

Cell	Slab	FEM Under-estimated Measured Curvature	FEM Over-estimated Measured Curvature	FEM and Measured Curvature Approximately Equal to FEM[1]
5	Restrained	4	1	0
	Unrestrained	5	1	0
6	Restrained	4	1	0
	Unrestrained	4	0	1
7	Restrained	3	2	1
	Unrestrained	3	3	0
8	Restrained	1	1	2
	Unrestrained	3	0	1
9	Restrained	4	0	1
10	Restrained	4	2	0
	Unrestrained	4	0	0
11	Restrained	4	1	0
	Unrestrained	4	1	1
12	Restrained	2	0	0
13	Restrained	5	0	1
	Unrestrained	3	0	3
Summary Statistics	Total	57	13	11
	Percentage	70%	16%	14%

[1]Curvatures were assumed approximate equal if they were within 20 percent of the curvature calculated using the measured profile.

Curvature was accurately determined using the FEM only 14 percent of the time. Measured curvatures that were accurately predicted using the FEM were between 2.5 x 10^{-4} 1/m (-7.6 x 10^{-5} 1/ft) and 2.8 x 10^{-4} 1/m (-8.5 x 10^{-5} 1/ft) for the restrained slabs and -3.5 x 10^{-4} 1/m (-1.1x 10^{-4} 1/ft) and 2.6 x 10^{-4} 1/m (-7.9 x 10^{-5} 1/ft) for the unrestrained slab. The FEM could not accurately estimate the larger curvatures that fell outside of these ranges.

The curvature data was also used to evaluate the ability of the FEM programs to predict curvature for slabs of different thickness, different restraint conditions (dowels and tie bars/no dowels and not tie bars) and different slab support conditions. Figures 8 and 9 show curvatures calculated for both the 190 mm (7.5 in) and 240 mm (9.5) slabs for the unrestrained and restrained slabs, respectively. Figure 10 compares the ability to estimate curvature for the 190 mm (7.5 in) slabs and 240 mm (9.5) slabs and figure 11 shows curvatures plotted for restrained slabs on a granular base and a stabilized base. These graphs are summarized in table 5. The curvatures calculated using slab profiles generated using the FEM tend to overestimate the curvatures calculated using measured profiles more frequently for thinner slabs and granular bases. Curvature was accurately estimated using FEM more frequently for unrestrained slabs than restrained slabs.

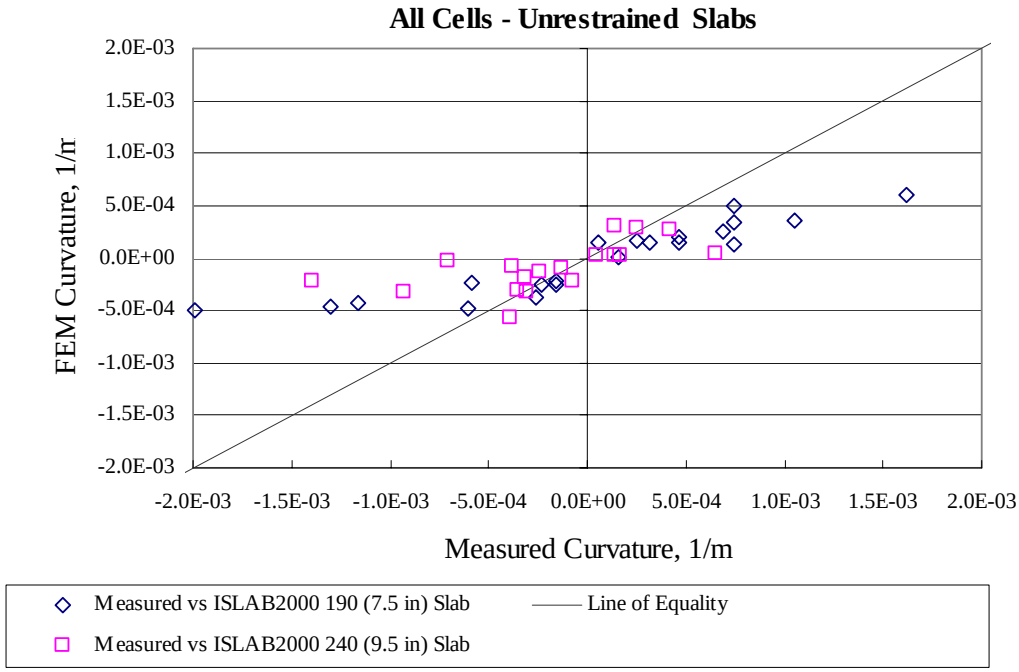

Figure 8. Curvatures of measured and finite element slab surface profiles for the unrestrained slabs in each test cell.

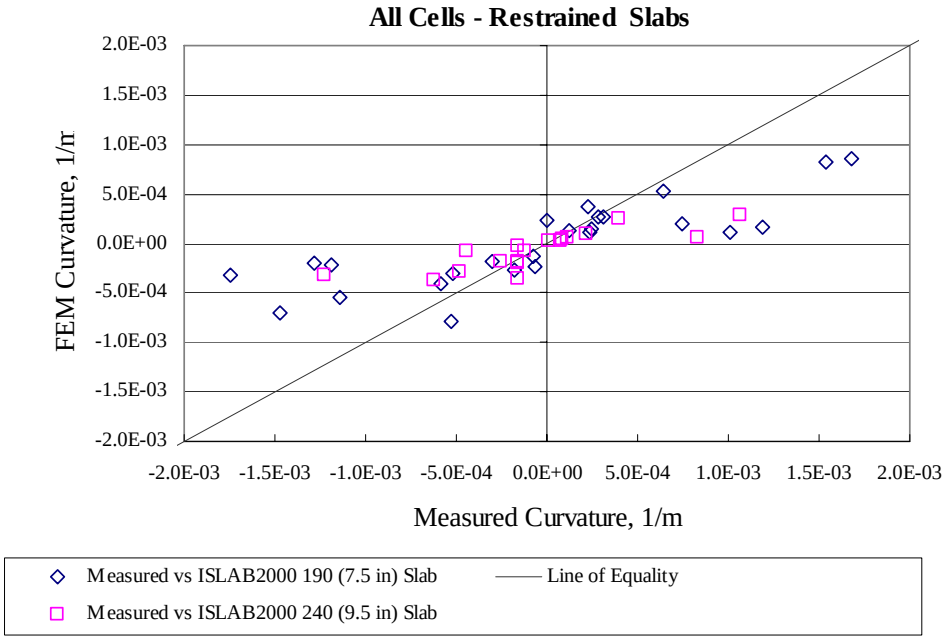

Figure 9. Curvatures of measured and finite element slab surface profiles for the restrained slabs in each test cell.

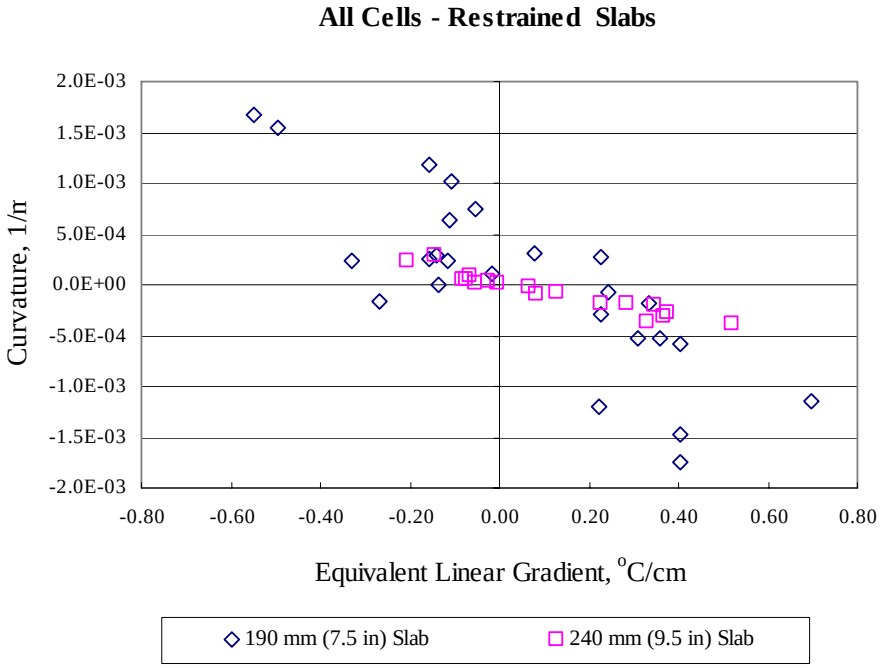

Figure 10. Curvatures of measured and finite element slab surface profiles plotted against the equivalent linear gradient under which it was measured for 190 mm (7.5 in) and 240 mm (9.5 in) slabs.

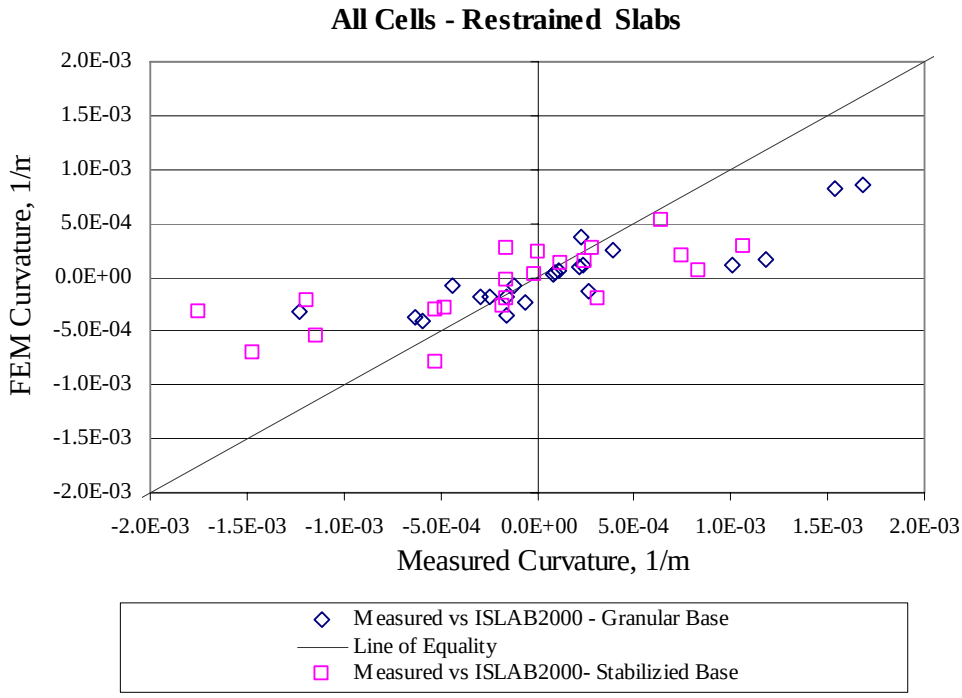

Figure 11. Curvatures of measured and finite element slab surface profiles for restrained slabs with different support conditions.

Table 5. Summary of FEM and measured profile curvatures for various design variables.

Cell	Design Variable	FEM Under-estimated Measured Curvature	FEM Over-estimated Measured Curvature	FEM and Measured Curvature Approximately Equal to FEM[1]
All Cells	190 mm slab	67%	20%	13%
	240 mm slab	74%	11%	14%
All Cells	Granular Base	63%	23%	14%
	Stabilized Base	67%	11%	13%
All Cells	Restrained	70%	18%	11%
	Unrestrained	70%	14%	16%

[1]Curvatures were assumed approximate equal if they were within 20 percent of the curvature calculated using the measured profile.

Conclusions

A comparison of the length of the unsupported portion of the slab determined using surface profile measurements and the FEM was performed. Only 12 percent of the FEM profiles were shifted upward from the measured slab profile, and therefore under-estimating the portion of the slab fully-supported. The shift in the profile was always less

than 500 microns (20 mils). All equivalent temperature gradients were greater than +0.28 °C/cm (+1.28 °F/in) for slabs approximately 190 mm (7.5 in) thick and greater than +0.52 °C/cm (+2.31 °F/in) for slabs approximately 240 mm (9.5 in) in thickness when this phenomena was exhibited.

The ability of the FEM to accurately estimate curvature appears to be a function of the pavement design and the magnitude of the gradient. The FEM was able to accurately predict curvature for several gradients in all cells but Cells 5, 10 and 12. Curvature was accurately determined using FEM only 14 percent of the time with curvature being under-estimated 70 percent of the time. The FEM is more likely to overestimate the curvature produce by a positive gradient than the curvature produced by a negative gradient. Measured curvatures that were accurately predicted using the FEM were between -2.5×10^{-4} 1/m (-7.6×10^{-5} 1/ft) and 2.8×10^{-4} 1/m (-8.5×10^{-5} 1/ft) for the restrained slabs and -3.5×10^{-4} 1/m (-1.1×10^{-4} 1/ft) and 2.6×10^{-4} 1/m (-7.9×10^{-5} 1/ft) for the unrestrained slab. The FEM could not accurately estimate the larger curvatures that fell outside of these ranges.

The curvatures calculated using slab profiles generated using the FEM tend to overestimate the curvatures calculated using measured profiles more frequently for thinner slabs and granular bases. The FEM predicted higher curvatures than were measured more frequently for the restrained slabs than the unrestrained slab.

Many speculations can be made in regards to reasons between the discrepancies between the measured and calculated slab response. It is evident that there is room for improvement in modeling the interaction between the bottom of the slab and the underlying layer as well as the restraint imposed by the dowel bar system. It was not surprising that the dense liquid foundation model employed tended to under predict curvature for the stablilized base more frequently than the unstabilized base. What was surprising was that it also under-estimated curvature more than 60% of the time for the unstabilized layer. This is an indication that improvements need to be made in modeling the base layer for both stabilized and unstabilized materials.

The 2002 rigid pavement design procedure developed under NCHRP 1-37A uses ISLAB2000 and neural network concepts to produce stress prediction equations for which transfer functions are developed. For this reason, it is critical that ISLAB2000 accurately model slabs loaded with a temperature gradient. This study has found that the FEM provides an accurate estimation of the portion of the slab supported by the base 88 percent of the time for the pavement designs included in this study. The FEM did underestimate the measured curvature 70 percent of the time. This results in underestimating slab stresses generated by temperature gradients. Fortunately, the development of transfer functions calibrated with field data will help to overcome the limitations in predicting stresses caused by temperature gradients.

Acknowledgments

The authors would like to gratefully acknowledge the Minnesota Department of Transportation and the Federal Highway Administration for their financial support. The authors would also like to thank Dr. Donald Janssen for his participation in this research effort and Mr. Matt Sheehan who directed the surface profile processing and measurement effort and who performed many of the surface profile measurements

himself. Ms. Sarah Schmidt's assistance in processing the surface profile measurements is also greatly appreciated along with the assistance of Mr. Jack Herndon, Mr. Robert Strommen, Mr. Gregory Larson and the personnel at the Mn/ROAD Research Facility. Finally, the authors would like to thank Mr. Aaron Fagerness for his assistance in performing the ISLAB2000 finite element runs.

References

1. *Minnesota Department of Transportation 1995 Specifications for Construction*, St. Paul, MN, 1995.

2. Face Company, *Dipstick Auto-Read Road Profiler Hardware Manual, Version 1.2*, Face construction Technologies, Inc., Norfolk, VA, June 1992.

3. Janssen, D. J. and M. B. Snyder, "Temperature Moment Concept for Evaluating Pavement Temperature Data" ASCE Journal of Infrastructure Systems, June 2000.

4. Vandenbossche, J. M., "*Interpreting Falling Weight Deflectometer Results for Curled and Warped Pavements*" Doctorate of Philosophy, Department of Civil and Environmental Engineering, University of Minnesota, Minneapolis, MN, 2003.

5. Khazanovich, L., H.T. Yu, S. Rao, K. Galasova, E. Shats, and R. Jones, ISLAB2000 - Finite Element Analysis Program for Rigid and Composite Pavements, User's Guide, ERES Consultants, Champaign, IL, 2000.

6. Wiseman, J. F., M. E. Harr and G. A. Leonards, "Warping Stresses in Concrete Pavements: Part II," *Highway Research Board Proceedings, Vol. 39,* Highway Research Board, Washington, DC, 1960.

7. Tarr, S. M., P. A. Okamoto, and M. J. Sheehan, "Concrete Pavement Warping, Curling and Subbase Interaction," Draft Report, Construction Technology Laboratories Inc., Skokie, IL, Oct. 1998.

8. Choubane, B. and M. Tia, "Nonlinear Temperature Gradient Effect on Maximum Warping Stresses in Rigid Pavements," Transportation Research Record 1370, Washington, DC, 1992.

9. Mirambell, E., "Temperature and Stress Distributions in Plain Concrete Pavements Under Thermal and Mechanical Loads," Second International Workshop on Design and Rehabilitation of Concrete Pavements, Siguenza, Spain, 1990.